

Anion-Binding Calixarene Receptors: Synthesis, Microstructure, and Effect on Properties of Polyether Electrolytes

A. Blazejczyk,[†] M. Szczupak,[†] W. Wieczorek,^{*,†} P. Cmoch,[‡] G. B. Appetecchi,[§]
B. Scrosati,[§] R. Kovarsky,^{||} D. Golodnitsky,^{||} and E. Peled^{||}

*Solid State Technology Division, Faculty of Chemistry, Warsaw University of Technology,
Noakowskiego 3, 00-664 Warsaw, Poland, Institute of Organic Chemistry, Polish Academy of Sciences,
Kasprzaka 44/52, 01-224 Warsaw, Poland, Department of Chemistry, University of Rome,
P-le A. Moro 5, 00-185 Rome, Italy, and Faculty of Exact Sciences, Tel-Aviv University,
Ramat Aviv, 69978 Tel Aviv, Israel*

Received August 10, 2004. Revised Manuscript Received December 16, 2004

In the present paper, a novel lithium-conducting polymer electrolyte, based on the low molecular weight dimethoxy poly(ethylene oxide) matrix as well as high molecular weight poly(ethylene oxide), is studied. New calixarene derivatives have been designed, synthesized, and successfully applied as neutral anion-binding receptors in the electrolytes, what could be of interest in the search for new sensors as well as for enhancing electrolytic functionality in energy-storage devices. Herein, details regarding synthesis and structural properties of all compounds incorporated in the polyether system are presented and discussed. The effect of supramolecular additives on physical (e.g., the charge-carriers transport mechanism, mechanical and thermal properties, or degree of crystallinity) and chemical (e.g., ion-receptor ion-matrix interactions) characteristics of polymer electrolyte is investigated in terms of differential scanning calorimetry, Fourier-transform IR spectroscopy, and impedance spectroscopy results. In particular, it was established that binding anions by some of the receptors under study may enhance ionic dissociation and after all increase the relative fraction of mobile lithium cations, leading to a transference number close to 1. Iodide anions complexing by the supramolecular additive were also found to be responsible for stabilization of the solid electrolyte–electrode interface. Its nature is discussed.

1. Introduction

The development of polymer electrolytes suitable for use in rechargeable lithium batteries represents one of the most important advances in technology since its introduction in the earliest 90s.¹ Up to now, most of the “Polymer Lithium-Ion Batteries” involve the use of a conventional liquid separator or gel-like electrolytes, and therefore, offer only limited advancement. There is still a great need for mechanical robust of a single lithium ion highly conductive polymer electrolyte of low toxicity and low cost.^{1,2} Intending to improve the characteristics of polymer electrolytes toward potential applications in electrochemical systems, various methods of modification have been applied.³ Most of these methods lead to an increase in ionic conductivity and some enhancement of cation transference number, what is of equal importance for the new generation devices performance. For instance, high efficiency of the lithium battery cell, beside high ionic mobility in electrolyte, also depends on electrode

reaction kinetics, i.e., on both the rate of electrochemically active ion charge transfer and the resistance of passive layers (usually formed on the lithium electrode surfaces), as these phenomena lead to the internal voltage drops in the battery. The battery improvement via enhancement of cationic transport and electrode kinetics can be observed in systems with higher cation transference number.

Armand et al. have shown that designing immobilized in matrix macro anions with the delocalized electrical charge (e.g., $\text{Al}[\text{Si}(\text{CH}_3)_2]^-$, $\text{B}(\text{C}=\text{C})_4^-$, $\text{SF}_5\text{CFHSO}_3^-$, $\text{SF}_5\text{CF}_2\text{SO}_3^-$, and $\text{N}(\text{SO}_2\text{PhNO}_2)_2^-$), which would have little or no power to complex cations, could be one of the most promising approaches.^{4,5} Unfortunately, that is also associated with relatively high cost and complicated synthesis of a salt used.

Among other methods of electrolyte modification, the use of inorganic fillers proved to be one of the most successful.^{6–15}

* All correspondence regarding this paper should be addressed to Prof. Władysław Wieczorek. Tel. + 48 22 6607572; fax + 48 22 628 2741; e-mail: wladek@ch.pw.edu.pl.

[†] Warsaw University of Technology.

[‡] Polish Academy of Sciences.

[§] University of Rome.

^{||} Tel-Aviv University.

- (1) Bruce, P. G. *Solid State Electrochemistry*; Bruce, P. G., Ed.; Cambridge University Press: Cambridge, UK, 1995.
- (2) Scrosati, B. *Applications of Electroactive Polymers*; Scrosati, B., Ed.; Chapman and Hall: London, 1993.
- (3) Gray, F. M. *Polymer Electrolytes*; Connor, J. A., Ed.; The Royal Society of Chemistry Materials Monographs, UK, 1997.

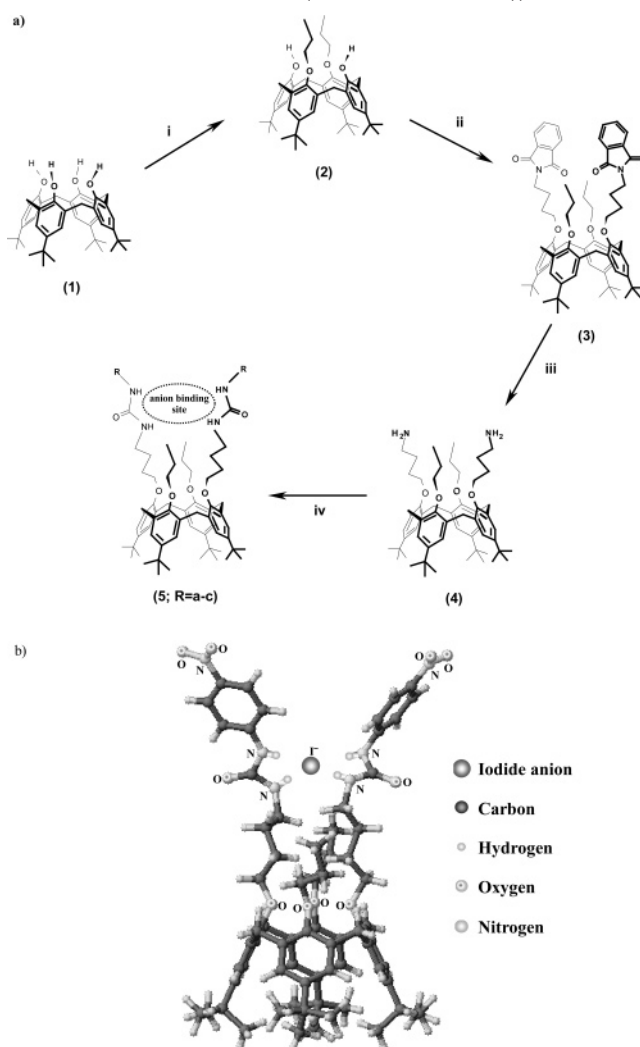
- (4) (a) Armand, M.; Gauthier, M. *High Conductivity Solid Ionic Conductors – Recent Trends and Applications*; Takahashi, T., Ed.; World Scientific Publication: Singapore, 1989; p 114. (b) Hael, N.; Nixon, P.; Gard, G.; Nafshun, R.; Lerner, M. *J. Fluorine Chem.* **1996**, 79, 81.
- (5) Alloin, F.; Bayaund, S.; Azimpour, B.; Reibel, L.; Sanchez, J. Y. *Electrochim. Acta* **1995**, 40, 2251.
- (6) Quartarone, E.; Mustarelli, P.; Magistris, A. *Solid State Ionics* **1998**, 110, 1.
- (7) Wieczorek, W.; Such, K.; Płocharski, J.; Wyciślik, H. *Solid State Ionics* **1989**, 36, 255.
- (8) Weston, J.; Steele, B. C. H. *Solid State Ionics* **1982**, 7, 81.
- (9) Fauteux, D. *J. Electrochem. Soc.* **1988**, 35, 2231.
- (10) Peled, E. *J. Electrochem. Soc.* **1979**, 126, 2047.
- (11) Peled, E.; Golodnitsky, D.; Ardel, G.; Eshkenazy, V. *Electrochim. Acta* **1995**, 40, 2197.

That may lead to both an increase in ionic conductivity⁷ and to improvement in thermal and mechanical stability.⁸ Moreover, it is supposed to limit the formation of passive layers at the interface.^{9–12} Scrosati et al. demonstrated that some improvement of electrolyte performance in the primary and secondary batteries can be realized by the addition of nanosized TiO₂ fillers.¹³

In the past decade, aiming to enhance cationic transport in polymer electrolyte, McBreen et al. provided another concept based on addition of an anion-complexing agent.¹⁶ Simultaneously, variations on the polymer electrolyte theme were interestingly pursued by Angel and co-workers, discussing the use of complexing species such as BEGs.¹⁷ Later, Metha and Fujinami prepared and tested polymer electrolytes incorporating boroxine rings with pendant oligoethers side chains and variety of dissolved lithium salts.¹⁸ Despite the fact that all the above-mentioned approaches led to an increase in the cationic transference numbers, the obtained values were still not close enough to unity.

Studies on the use of anion receptors in polymer electrolytes are very limited. So far, mostly cationic receptors such as crown ethers, cryptands, and calixarenes have been used in low molecular weight nonaqueous solutions^{19–21} or in polymer electrolytes.¹ To our knowledge, papers dealing with this subject based on either theoretical predictions^{22,23} or fundamental studies, i.e., on addition of boron family compounds applied into solutions of lithium salts in both aprotic (inert) electrolytes of low molecular weight solvents²⁴ and gel polyelectrolytes,²⁵ as well as studies on linear or cyclic aza-ether compounds (with electron-withdrawing groups) incorporated into oligoethers^{16,26} or grafted directly

Scheme 1. Synthesis of Urea *p*-tert-Butylcalix[4]arene Derivatives with Different Substituents (R) (There Is the Anion Binding Site Indicated in the Resulting Macromolecules (5a–c Shown Below))



- (12) Croce, F.; Curini, R.; Martinello, A.; Persi, L.; Ronci, F.; Scrosati, B.; Caminiti, R. *J. Phys. Chem.* **1999**, *103*, 10632.
- (13) Croce, F.; Appetecchi, G. B.; Perci, L.; Scrosati, B. *Nature* **1998**, *394*, 456.
- (14) Wiczonek, W.; Lipka, P.; Żukowska, G.; Wyciślik, H. *J. Phys. Chem. B* **1998**, *102*, 6968.
- (15) Wiczonek, W.; Florjańczyk, Z.; Stevens, J. R. *Electrochim. Acta* **1995**, *40*, 2251.
- (16) (a) Lee, H. S.; Yang, X. Q.; McBreen, J.; Choi, L. S.; Okamoto, Y. *Electrochim. Acta*, **1995**, *40* (13–14), 2353. (b) Lee, H. S.; Yang, X. Q.; McBreen, J.; Choi, L. S.; Okamoto, Y. *J. Electrochem. Soc.* **1996**, *143* (12), 3825.
- (17) (a) Angell, C. A.; Xu, K.; Zhang, S.-S.; Videa, M. *Solid State Ionics* **1996**, *86–88*, 17–28. (b) Zhang, S.-S.; Angell, C. A. *J. Electrochem. Soc.* **1996**, *143*, 4047.
- (18) Metha, M. A.; Fujinami, T. *Chem. Lett.* **1997**, *916*, 4047.
- (19) (a) Matsuda, Y.; Hayashida, H.; Morita, M. *J. Electrochem. Soc.* **1987**, *134*, 2107. (b) Danil de Namor, A. F.; Llosa Tanco, M. A.; Salomon, M.; Ng, J. C. Y. *J. Phys. Chem.* **1994**, *98*, 11796. (c) Danil de Namor, A. F.; Llosa Tanco, M. A.; Salomon, M.; Ng, J. C. Y. *J. Phys. Chem.* **1996**, *100*, 14485.
- (20) Danil de Namor, A. F.; Pulcha Salazar, L. E.; Llosa Tanco, M. A.; Kowalska, D.; Salas, J. V.; Schulz, R. A. *J. Chem. Soc., Faraday Trans.* **1998**, *94*, 3111.
- (21) Danil de Namor, A. F.; Hutcherson, R. G.; Verlade, F. J. S.; Ormachera, M. L. Z.; Salazar, L. E. P.; Jammaz, I. A.; Rawi, N. A. *Pure Appl. Chem.* **1998**, *70*, 769.
- (22) Johansson, P. *Electrochim. Acta* **2003**, *48* (14–16), 2291.
- (23) Johansson, P.; Jacobsson, P. *Electrochim. Acta* **2004**, in press.
- (24) (a) Lee, H. S.; Yang, X. Q.; Xiang, C. L.; McBreen, J.; Choi, L. S. *J. Electrochem. Soc.* **1998**, *145*, (8) 2813. (b) Sun, X.; Lee, H. S.; Lee, S.; Yang, X. Q.; McBreen, J. *Electrochem. Solid State Lett.* **1998**, *1* (6), 239.
- (25) Zhou, F.; MacFarlane, D. R.; Forsyth, M. *Electrochim. Acta* **2003**, *48* (12), 1749.
- (26) (a) McBreen, J.; Lee, H. S.; Yang, X. Q.; Sun, X. *J. Power Sources* **2000**, *89*, 163. (b) Lee, H. S.; Yang, X. Q.; Sun, X.; McBreen, J. *J. Power Sources* **2001**, *97–98*, 566.

^a Reagents and conditions: **i**, *n*-C₃H₇I, K₂CO₃, (CH₃)₂CO, ΔT; **ii**, C₁₂H₁₂BrNO₂, NaH, DMF, 70–75 °C; **iii**, N₂H₄·H₂O, EtOH/THF, ΔT; **iv**, R(a-c)-NCO, CHCl₃, r.t.

to polymer chains.²⁷ This paper aims at describing a step further toward development of a new single ion-conducting polymer electrolyte. Significant enhancement up to nearly 100% of the Li⁺ charge transference (through a symmetric cell with lithium electrodes), in addition to evidently improved electrode–electrolyte interface performance, is presented herein as obtained by using anion-binding supramolecular components, namely, calix[4]arene R-urea derivatives (with R = phenyl, *t*-butyl, *p*-nitrophenyl; see Scheme 1), in the role of additives for the solid poly(ethylene oxide)–lithium salt (PEO)–LiX blends (where X stands for I⁻ or CF₃SO₃⁻).

More precisely, the main aim of our work was to analyze the R-dependent calixarene anion-receptor type and its concentration (in respect to dopant salt) effect on ionic transport and microstructure of the composite lithium–polyether electrolytes. To do that, three calixarene com-

- (27) Lee, H. S.; Yang, X. Q.; Xiang, C. L.; McBreen, J.; Callahan, J. H.; Choi, L. S. *J. Electrochem. Soc.* **1999**, *146* (3), 941.

pounds (of various complexing abilities) were synthesized and added to low and high molecular weight polyether electrolytes. The liquid dimethoxy poly(ethylene oxide)–lithium iodide, P(EO)DME–LiI, was examined in the first place. That allowed finding out some important chemical features of the ionic-conducting polymer electrolyte system involving anion receptors, either on macro- or microscopic levels.

Ionic conductivity and lithium electrolyte–electrode transference number t_+ were studied by means of impedance spectroscopy (IS) combined with direct current (ac/dc) measurements as a function of salt concentration and fraction of added calixarene receptors. The anion–calixarene and cation–matrix interactions were analyzed using Fourier-transform IR (FTIR) measurements. Additionally, study on polymer chain flexibility was carried out by means of differential scanning calorimetry (DSC).

The effect of type of receptor used is discussed on the basis of molecular modeling, t_+ determination, as well as studies on the formation and time performance of the electrode–electrolyte interfacial solid electrolyte interface (SEI) layers.

The details of explanation why we have chosen the calixarene receptors as additives in polymer electrolytes are included in Appendix 1.

2. Experimental Section

2.1. Synthesis of the Calix[4]arene Derivatives. The synthesis course is illustratively presented in Scheme 1. The starting compounds **1**²⁸ and **2**²⁹ were obtained accordingly to procedures previously described in the literature. The compounds **3** and **4** were obtained along with the preparation procedures given in section 2.1.1. The way of synthesizing the compound **5a** is explained in section 2.1.2. The procedure differed from that described in the literature.^{30,31} The main difference was to use the compound **3** as a half product in the synthesis. That resulted in a quadruple increase of the total process yield and enabled obtaining larger fractions of end products. Both final compounds **5b** and **5c** were synthesized for the first time, in a similar way as the compound **5a** in this study.

All reactions, except the synthesis of compounds **1** and **4**, were carried out under the protection of an argon atmosphere. Separation and purification of compounds **3** and **5a–c** were made by flash column chromatography (FCCh) at the pressure of approximately 0.1 atm. Silica gel 60 (particle size 0.04–0.063 mm, 230–240 mesh) was obtained from Merck. The progress of reactions was controlled by thin-layer chromatography (TLC) on plastic plates covered with a 0.2-mm-thick layer of silica gel 60 F254, manufactured by Merck. To complete the procedure, the organic phase was washed solely with distilled water and, depending on needs, either acidified with a water solution of 1 N HCl or alkalized with 1 N NH₃ (for compound **4**) and dried over MgSO₄.

The typical solvents required in due course of the synthesis, CHCl₃ and CH₂Cl₂, were distilled over CaCl₂ and stored over molecular sieves type 4 Å for 3 days. The solvents together with C₆H₅CH₃ (toluene) and other chemicals, *t*-C₄H₉C₆H₄OH (*p*-*tert*-butylphenol), HCHO, 37 wt. % aq. (formaldehyde), NaOH, C₃H₇I (propyl iodide), K₂CO₃, C₆H₅NCO, *t*-C₄H₉NCO, and *p*-C₆H₄NCO (phenyl, *tert*-butyl, and *p*-nitrophenyl isocyanates), were of reagent grade and used without further purification. The analytical-grade quality reagents, DMF (*N,N*-dimethylformamide) (anhydrous 99.8%); EtOH (ethyl alcohol) (anhydrous 99.9%), and acetone (anhydrous 99.9%), were obtained from Aldrich and NaH, used as 55% suspension in oil, were supplied by Fluka.

To identify, all compounds **1–5** were subsequently characterized by melting point, NMR, IR, and MS testing measurements, including microanalysis. Before the chemical analysis, they were dried under reduced pressure of $\sim 10^{-5}$ Torr at 50 °C for 8 h except the compound **1** dried at 145 °C for 35 h.

The melting point of compounds was determined with the capillary melting-point apparatus in a vacuum sealed capillary tubes (under 10^{-3} Torr) and in all cases exceed 200 °C. The results for **1**,²⁸ **2**,^{29a} **4**,³⁰ and **5a**³⁰ differ from those quoted in the literature.

The ¹H NMR and ¹³C NMR spectra of compounds in the form of solutions in CDCl₃ were measured using Varian Mercury 400BB (400 MHz) and Varian Unityplus 500 (500 MHz) spectrometers. The obtained coupling constant values (*J*) are given in Hz. Chemical shifts (δ) are given in ppm in relation to (CH₃)₄Si as the internal standard. In description of spectra, the following abbreviations are used: s, singlet; d, doublet; t, triplet; q, quartet; sept, septet; m, multiplet. The ¹H NMR and ¹³C NMR spectra of **1**,^{32,33} **2**,²⁹ **4**,³⁰ and **5a**³⁰ compounds were identical with those previously described.

FTIR spectra were recorded on a computer-interfaced Perkin-Elmer 2000 FTIR system in the transmittance mode, with the wavenumber resolution of 2 cm⁻¹ in the frequency range of 600–4000 cm⁻¹ in KBr pellets.

Mass spectra were obtained by both MALDI-TOF (matrix-assisted laser desorption and ionization time-of-flight) and ESI (electrospray ionization) techniques. MALDI-TOF mass spectra were acquired using a Kratos Analytical Compact MALDI 4 V5.2.1 mass spectrometer equipped with a 337-nm nitrogen laser with a 3-ns pulse duration. The measurements were carried out in linear mode at the acceleration voltage of the instrument set at 20 kV. For each sample, spectra were averaged out of 200 laser shots. The samples were dissolved in THF (tetrahydrofuran) and CHCl₃ using DHB (2,4-dihydroxybenzoic acid) as a matrix. To avoid distortions of the signal, the laser power was moderated in the range of 30–65 units characteristic for the type of measurement. ESI mass spectra were acquired with a MARINER ESI time-of-flight mass spectrometer (PerSeptive Biosystem) with the resolution of 5000 (full width at half maximum). The needle voltage was 3.5 kV, and the inlet capillary temperature was maintained at 140 °C. The declustering potential varied from 80 to 140 V, depending on the type of experiment. All the spectra were collected in the positive ion mode. Sample solutions were prepared by mixing the compound with a mixture of solvents: MeOH (methyl alcohol) and CH₂Cl₂. The calculations of molecular mass of compounds were performed using the ACDLabs 5.0/ChemSketch software.

Microanalyses were acquired using Perkin-Elmer PE Serial II CHNS/O.

- (28) (a) Gutsche, C. D.; Iqbal, M.; Stewart, D. *J. Org. Chem.* **1986**, *51*, 742. (b) Gutsche, C. D.; Iqbal, M. *Org. Synth. Coll.* Vol. VIII, 75. (c) Gutsche, C. D.; Dhawan, B. D. *J. Am. Chem. Soc.* **1981**, *103*, 3782. (29) (a) Iwamoto, K.; Yanagi, A.; Araki, K.; Shinkai, S. *Chem. Lett.* **1991**, 473. (b) Iwamoto, K.; Araki, K.; Shinkai, S. *Tetrahedron* **1991**, *47*, 4325. (c) Iwamoto, K.; Fujimoto, K.; Shinkai, S. *Tetrahedron Lett.* **1990**, *31*, 7169. (30) Scheerder, J.; Fochi, M.; Engbersen, J. F. J.; Reinhoudt, D. N. *J. Org. Chem.* **1994**, *59*, 7815. (31) Kenis, P. J. A.; Noordman, O. F. J.; van Hulst, N. F.; Engbersen, J. F. J.; Reinhoudt, D. N. *Chem. Mater.* **1997**, *9*, 596.

- (32) Kammerer, H.; Happel, G.; Caesar, F. *Makromol. Chem.* **1972**, *162*, 179. (33) Gutsche, C. D. *Calixarenes*; Stoddart, J. F., Ed.; The Royal Society of Chemistry: Cambridge, UK, 1998.

For comparison, the corresponding data (^1H NMR, ^{13}C NMR, IR, MS, Anal. Calcd, mp) obtained in this study are listed in the Appendix 2.

2.1.1. Preparation Procedure of the Calix[4]arene Derivatives (3) and (4). 5,11,17,23-Tetra-*p*-*tert*-butyl-25,27-bis[(*N*-4-phthalimidobutyl)oxy]-26,28-dipropoxycalix[4]arene (**3**). The sodium salt solution of compound **2** (6.48 g, 8.84 mmol) received in the presence of NaH (1.3 g, 29.8 mmol) in DMF (100 mL) was prepared in a separate vessel. The whole solution was well stirred until complete dissolution at room temperature. Next, the mixture was carefully instilled into the solution of dissolved in DMF (55 mL), the *N*-(4-bromobutyl)phthalimide (11.8 g, 41.82 mmol) agent, prepared before by using the Salzberg–Supniewski method.³⁴ After about 3 h, temperature of the reactive mixture was set up to 75 °C, and the mixture was stirred for 24 h. The reaction course was monitored in situ by means of TLC (SiO_2 ; CHCl_3 :MeOH = 99:1 or CHCl_3). After cooling to room temperature and adding 5 mL of H_2O , the DMF was evaporated under reduced pressure ($\sim 10^{-3}$ Torr). The residue (ca. 16 g) was dissolved in CHCl_3 (250 mL) and subjected to the standard procedure (mentioned above). After drying over MgSO_4 , the organic solvent was vaporized to dryness. The product **3** was separated from the solid residue via FCCh. By use of eluents in the following order: CH_2Cl_2 :hexane = 1:1, CHCl_3 and CHCl_3 :MeOH = 9:1, FCCh enabled the production of pure **3** as a white powder in 60% reaction yield.

5,11,17,23-Tetra-*p*-*tert*-butyl-25,27-bis[(4-aminobutyl)oxy]-26,28-dipropoxycalix[4]arene (**4**). A suspension of compound **3** (6 g, 5.28 mmol) in THF (100 mL) and EtOH (400 mL) was refluxed for 5 h after adding hydrazine monohydrate (8 g, 128 mmol, 80% aq) and stirred intensively at room temperature for 24 h. The reaction was carried out until the substrate was fully exhausted. The progress of the reaction was monitored by means of TLC (SiO_2 ; CHCl_3 :MeOH = 99:1 or CHCl_3). Upon cooling of the transparent solution, a white precipitate (phthalide acid hydrazide) was formed. The precipitate was filtered off. The filtrate was concentrated in vacuo; CHCl_3 (400 mL) was added into the filtrate, and the whole mixture was subjected to the standard procedure (as above). After drying over MgSO_4 , the organic solvent was evaporated. That resulted in a yellowish oil, compound **4**, that was dried ($\sim 10^{-3}$ Torr, 40 °C, 3 h) subsequently. Compound **4** was obtained as a light yellow powder in 86% reaction yield.

2.1.2. Preparation Procedure of the Calix[4]arene R-Urea Derivatives (5). 5,11,17,23-Tetra-*p*-*tert*-butyl-25,27-bis[*N'*-fenylureido)butyl]oxy]-26,28-dipropoxycalix[4]arene (**5a**) with *R* = phenyl, 5,11,17,23-Tetra-*p*-*tert*-butyl-25,27-bis[*N'*-*tert*-butylureido)butyl]oxy]-26,28-dipropoxycalix[4]arene (**5b**) with *R* = *tert*-butyl, and 5,11,17,23-Tetra-*p*-*tert*-butyl-25,27-bis[*N'*-*p*-nitrofenylureido)butyl]oxy]-26,28-dipropoxycalix[4]arene (**5c**) with *R* = *p*-nitrophenyl. In all cases, 10.12 mmol of isocyanate (corresponding to **5a–c** in Scheme 1) was added to 4.57 mmol of compound **4** dissolved in CHCl_3 (120 mL). The solution was stirred for 24 h at ambient temperature. The reaction was performed until full exhaustion of the substrate. Its progress was monitored by means of TLC (SiO_2 ; CH_2Cl_2 :MeOH = 98:2). Once the process was completed, only H_2O (150 mL) was added. The next step was to separate and dry the organic layer over MgSO_4 . The organic solvent was evaporated, and the crude products were purified as described.

5a: washed with methanol, purified using FCCh (SiO_2 ; CH_2Cl_2).

5b: recrystallized from methanol, purified using FCCh (SiO_2 ; CH_2Cl_2 :MeOH 98:2).

5c: washed with methanol, purified using FCCh (SiO_2 ; CH_2Cl_2 :MeOH 98:2).

The corresponding reaction resulted in: **5a** (white powder), 85%; **5b** (white powder), 72%; and **5c** (yellow powder), 91%.

2.2. Electrolyte Preparation. All the procedures of electrolyte preparation have been carried out in an argon-filled drybox with moisture content lower than 10 ppm. Before electrolyte composition, all ingredients, except anhydrous salts LiI and LiCF_3SO_3 (99.999%, Aldrich, reagent grades), were dried separately under reduced pressure (ca. 10^{-5} Torr) on a vacuum line. Calix[4]arene R-urea derivatives were dried at 50 °C for 20 h and P(EO) ($M_w = 5 \times 10^6$, Aldrich, reagent grade) at 50 °C for 24 h. The liquid P(EO)-DME ($M_w = 500$, Aldrich, reagent grade) was filtered and carefully freeze-dried, using 4 freeze–pump–thaw cycles, before being dried at 45 °C for 50 h. The solvent used in preparation of the solid electrolytes, CH_3CN (acetonitrile, Lab Scan Ltd, for analysis), was meticulously freeze-dried and double distilled over molecular sieves type 4 Å.

2.2.1. P(EO)DME-Based Liquid Electrolyte Preparation. The chemical compositions of liquid electrolytes were chosen as the following: $\text{P(EO)DME}_{100}(\text{LiI})_1(\text{5a})_x$ and $\text{P(EO)DME}_{10}(\text{LiI})_1(\text{5a})_x$ for calixarene molar ratio in respect to salt from $x = 0$ to $x = 0.8$. The LiI salt was dissolved in P(EO)DME polymer matrix using a magnetic stirrer. Concentration of the salt with respect to oxirane monomeric units (O:Li ratio) varied from 100:1 to 10:1. All electrolytes were prepared by direct dissolution of the salt in the polymer. Next, appropriate amounts of solution were placed in glass vessels, and the calixarene was carefully added in proper proportions. To facilitate dissolution, samples with the highest salt and calixarene concentrations were warmed to 35 °C. All electrolyte samples were equilibrated in a drybox at ambient temperature before being used in any experiments.

2.2.2. P(EO)-Based Solid Electrolyte Preparation. The chemical composition was chosen as $\text{P(EO)}_y(\text{LiI})_1(\text{5a–c})_x$ for calixarene molar ratio in respect to salt from $x = 0$ to $x = 0.8$, $y = 100, 20, 10, 7$. The LiI salt was added into P(EO) solution in CH_3CN (40 mL) and homogenized by magnetic stirring at ambient temperature in the argon-filled drybox. Next, calixarene ingredient was added, and the mixture was stirred again until homogenization. In the case of **5a** for $x > 0.6$ ($y = 10$) and **5b** for $x > 0.3$ ($y = 7$), samples did not reveal complete solubility. The mixture was cast on Teflon plates. The excessive amount of CH_3CN was evaporated for 24 h under vacuum at ambient temperature. Next, solvent-free films were dried at 45 °C for 60 h. Before measurements, all the samples were stored in a drybox at ambient temperature, until they reached intrinsic crystallization in the electrolyte.

2.3. Electrolyte Samples Characterization. **2.3.1. DSC Thermal Analysis.** Thermal analysis was conducted to measure glass transition (T_g) and melting (T_m) temperatures. DSC experiments were performed on a Perkin-Elmer Pyris 1 scanning calorimeter equipped with a low-temperature measuring head and a liquid nitrogen cooled heating element. Samples in aluminum pans were loaded into a drybox under N_2 atmosphere and stabilized by slowly cooling them down to -150 °C and then heating at 20 °C/min to 70 °C. The temperature scale was calibrated with the melting point of indium. In all scans, empty aluminum pans were used as a reference. The estimated error in the determination of T_g and T_m was ± 2 °C.

2.3.2. Conductivity Measurements. Ionic conductivity at 0–70 °C of liquid and 0–90 °C of solid electrolytes was determined by means of IS. Liquid electrolytes were placed in a constant-volume cylindrical cell of 1.6-mm thickness with two symmetrical 7.8-mm-diameter electrodes. Solid electrolytes in the form of disks were pressed between stainless steel blocking electrodes of 8 mm in

(34) (a) Salzberg, P. L.; Supniewski, J. V. *Org. Synth. Coll.*, 2nd ed.; John Wiley and Sons: New York, 1941, Vol. 1, p 119. (b) Mizzone, R. H.; Hennessey, M. A.; Scholz, C. R. *J. Am. Chem. Soc.* **1954**, *76*, 2414. (c) Cope, A. C.; Nace, H. R.; Hatchard, W. R.; Jones, W. H.; Stahmann, M. A.; Turner, R. B. *J. Am. Soc.* **1949**, *71*, 554.

Table 1. Values of Activation Energy for Ionic Conduction Calculated from the Arrhenius-Type Eq 2 for the Homogeneous P(EO)₁₀(LiI)(Calixarene)_x Solid Electrolytes

<i>x</i> ratio ^a	<i>E</i> _{a1} ^b /eV	<i>E</i> _{a2} ^c /eV	<i>E</i> _m ^d /eV	<i>E</i> _c ^e /eV
0	2.19	0.51	0.51	1.68
0.05	1.14	0.59	0.59	0.55
0.10	1.30	0.60	0.60	0.70
0.20	1.11	0.63	0.63	0.48
0.40	1.10	0.62	0.62	0.48

^a Calixarene **5a** in respect to LiI salt molar concentration. ^b *E*_{a1}: activation energy for the conduction below the melting point of the crystalline phase. ^c *E*_{a2}: activation energy for the conduction above the melting point of the crystalline phase. ^d *E*_m: activation energy for migration, assumed to be equal to *E*_{a2}. ^e *E*_c: activation energy for the charge carrier creation calculated as *E*_c = *E*_{a1} − *E*_{a2}.

Table 2. *T*_g Values for Solid Polyether–LiI–Calixarene Electrolytes

polyether	O:Li ratio ^a	<i>x</i> ratio ^b	<i>T</i> _g /K
P(EO)DME	no salt	no additive	187
P(EO)DME	100	no additive	199
P(EO)DME	100	0.02	203
P(EO)DME	100	0.05	209
P(EO)DME	100	0.20	211
P(EO)DME	10	no additive	230
P(EO)DME	10	0.02	229
P(EO)DME	10	0.05	225
P(EO)DME	10	0.10	219
P(EO)	no salt	no additive	214
P(EO)	10	no additive	251
P(EO)	10	0.05	240
P(EO)	10	0.10	239
P(EO)	10	0.20	238

^a Oxirane monomeric units in respect to salt molar concentration. ^b Calixarene **5a** in respect to LiI salt molar concentration.

diameter. Their thickness ranged from 150 to 330 μm. The measuring cells were evacuated (~10^{−5} Torr) for 2 h prior to the experiments. The measurements were carried out on a PC-controlled Solatron-Schlumberger 1255 impedance analyzer over the frequency range of 1–100 kHz. The experimental data were analyzed using the complex nonlinear least-squares fitting (CNLS) procedure, developed by Boukamp³⁵ to determine the direct current conductivity of samples. The reproducibility of the IS results was checked in the multiple experiments, performed in overall temperature range. The samples before measurements were thermostated for 0.5 h. Because of the temperature gradient between the thermocouple and the sample, its temperature could not be determined with a better accuracy than ±2 °C.

2.3.3. Determination of the Lithium Ion Transference Number. The lithium ion transference number (*t*₊) of the membrane samples was measured between 50 and 90 °C for various contents of calixarene and salt in the polymer electrolyte system. The steady-state technique, which involves a combination of ac and dc measurements, was applied. The impedance response of the Li//solid–electrolyte//Li cell was measured prior to the dc-polarization run, in which a small voltage pulse (Δ*V*) was applied to the cell until the polarization current reached the steady-state *I*_{ss} (after 2 or 3 h at 90 or 50 °C, respectively). Various voltage pulses (3–30 mV) were applied in order to test the experimental error, which did not exceed 10% in determination of transference numbers *t*₊. Finally, the impedance response of the cell was measured again. The double IS test is required to determine electrolyte resistance (*R*_e) as well as the SEI resistance before (*R*₀) and after (*R*_{ss}) dc polarization. That allowed evaluation of usually great difficulty to determine initial current (*I*₀) arising immediately (~10 μs at 50 °C) after appli- cation of the voltage, since, along with the Ohm's law, *I*₀ = Δ*V*/(*R*_e + *R*₀).

Table 3. DSC Data for Solid Polyether–Calixarene System without Salt

polyether	<i>x</i> ratio ^a	<i>T</i> _g /K	<i>T</i> _m /K	<i>Q</i> _m /Jg ^{−1}	<i>X</i> _c (%)
P(EO)	0	214	343.15	137	64
P(EO)	0.05	215	339.25	131.1	61.3
P(EO)	0.10	216	338.55	123.6	57.8
P(EO)	0.20	217	338.25	96.3	45.1
P(EO)	0.40	218	339.25	94.3	44.1
P(EO)	0.60	219	338.55	63.9	29.9
P(EO)	0.80	219	337.85	59.6	27.9

^a Calixarene **5a** in respect to LiI salt molar concentration.

Table 4. FTIR Data for Liquid and Solid Polyether–LiI–Calixarene Electrolytes

polyether	O:Li ratio ^a	<i>x</i> ratio ^b	C–O–C max/cm ^{−1}	NH max/cm ^{−1}
P(EO)DME	no salt	no additive	1112	
P(EO)DME	100	no additive	1107	
P(EO)DME	100	0.02	1108	3251
P(EO)DME	100	0.05	1108	3253
P(EO)DME	100	0.20	1109	3256
P(EO)DME	10	no additive	1093	
P(EO)DME	10	0.02	1094	3254
P(EO)DME	10	0.05	1095	3278, 3247
P(EO)DME	10	0.10	1096	3287, 3261

^a Oxirane monomeric units in respect to salt molar concentration.

^b Calixarene **5a** in respect to LiI salt molar concentration.

Table 5. Lithium Ion Transference Number *t*₊ for Solid P(EO)_y(LiI)₁(Calixarene)_x and P(EO)_y(LiCF₃SO₃)₁(Calixarene)_x Polymer Electrolytes as a Function of Temperature or Salt and Calixarene Content

additive	salt	<i>t</i> /°C	O:Li ratio ^a	<i>x</i> ratio ^b	<i>t</i> ₊
calixarene 5a	LiI	90	100	0	0.14
		90	100	0.25	0.15
		90	100	0.50	0.18
		50	20	0	0.35
		50	20	0.30	0.59
calixarene 5b	LiI	50	20	1.00	0.36
		75	7	0	0.56
		75	7	0.30	0.70
calixarene 5c	LiCF ₃ SO ₃	60	20	0	0.26
		60	20	1.00	0.90
	LiI	90	7	0.30	0.69
		75	7	0.30	0.74
		55	20	0.30	0.51
		90	20	1.00	0.80
		75	20	1.00	0.93
		50	20	1.00	1.00

^a Oxirane monomeric units in respect to salt molar concentration.

^b Calixarene content in respect to LiI salt molar concentration.

According to this method,³⁶ the transference number *t*₊ of lithium ions, as the carriers of charge flowing through the entire Li//polymer–electrolyte//Li cell, thus including bulk and interfacial resistances, could be calculated with the following workable equation

$$t_+ = \frac{I_{ss}(\Delta V - I_0 R_0)}{I_0(\Delta V - I_{ss} R_{ss})} = \frac{R_e}{\frac{\Delta V}{I_{ss}} - R_{ss}} \quad (1)$$

where *R*₀ is the initial SEI resistance of passive layers formed at both lithium electrodes and *R*_{ss} is the secondary passive layer resistance (as the steady-state polarization current is reached).

All the *t*₊ values obtained based on eq 1 are collected in Table 5.

2.3.4. FTIR Spectroscopy. Middle IR spectra were recorded in the transmittance mode on a PC-interfaced Perkin-Elmer 2000 FTIR system with the wavenumber resolution of 2 cm^{-1} in the $600\text{--}4000\text{-cm}^{-1}$ frequency range. FTIR studies were performed at $25\text{ }^{\circ}\text{C}$. Electrolytes were sandwiched between two NaCl plates in a drybox under N_2 atmosphere and were transferred into the FTIR chamber with controlled temperature. The accuracy of the sample's temperature measurement was $\pm 1\text{ }^{\circ}\text{C}$. A Galactic Grams 386 software package was used to analyze the FTIR data.

3. Results

3.1. IS, DSC, and FTIR Characteristics of the Composite Polymer Electrolytes. Figure 1 presents the conductivity isotherms obtained at 15, 40, and $70\text{ }^{\circ}\text{C}$ for P(EO)-DME-based electrolytes as a function of calixarene **5a** concentration for samples containing various amounts of LiI (expressed as O:Li ratios). Generally, the addition of calixarene (at O:Li constant) results in a decrease in the total ionic conductivity (even below 10^{-5} S cm^{-1}), reflecting the complexing phenomenon. An increase in salt concentration (at x constant) gives rise to a local maximum (well above 10^{-3} S cm^{-1} at $70\text{ }^{\circ}\text{C}$, $x = 0$). By addition of calixarene receptors, the maximum shifts toward lower salt concentrations (see dashed lines on parts a and b of Figure 1) except the highest temperature ($70\text{ }^{\circ}\text{C}$), where the tendency is opposite (Figure 1c). From a macroscopic point of view, the occurrence of the total conductivity local maxima vs salt concentration reflects a natural limit of its chemical solubility and dissociation in polymer matrix. Microscopically, it is related to unavoidable ionic association developing with an increase in concentration. On the basis of the Fuoss–Kraus calculations,³⁷ one may conclude that, in the range where conductivity increases, the contribution of free ions decreases while a population of positively charged triplets develops.^{38–40} The trend breaks most probably when triplets aggregate into more complex multiplets and macroscopic viscosity effect is predominant.

It is worthy to note that at highest salt concentration (O:Li < 20) and lower temperature range calixarene causes increase in conductivity of the electrolyte, evidenced as local maximum (Figure 1a). The position of this maximum shifts to the higher salt concentration range with an increase in temperature. That is one of important evidences for positive acting and usefulness of this agent in electrolyte, since, when iodide anion is being complexed, two free cations might be released from a positively charged triplet, or even more, from a multiplets. The same phenomenon occurs in solid-state polymer electrolytes (see Figure 4b).

Changes in the conductivity as a function of reciprocal temperature for P(EO)DME-based electrolytes with the O:Li ratio equal to 100:1 and 10:1, containing various amounts of calixarene, are shown in Figures 2 and 3, respectively. For 100:1 electrolytes, the conductivity decreases with an

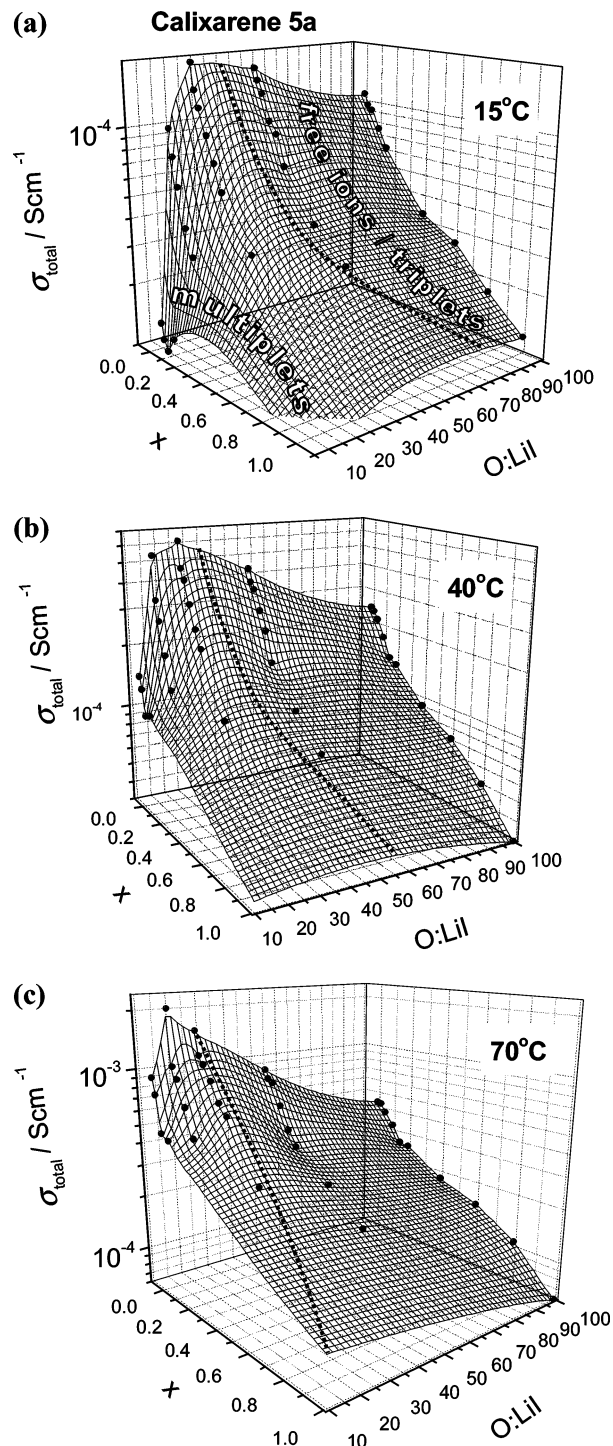


Figure 1. Conductivity isotherms of the system $\text{P(EO)DME}_x(\text{LiI})_{1-x}$ (calixarene) $_x$ as a function of calixarene content and amount of salt expressed by O:Li ratio at various temperatures. The apparent conductivity changes are hypothetically assigned to changes of the charge carriers type in the system (from free ions and triplets toward multiplets).

increase in the calixarene concentration over the entire temperature range. For 10:1 electrolytes, at temperatures below $30\text{ }^{\circ}\text{C}$, the conductivity increases with calixarene concentration. At higher temperatures, trends similar to those of the 100:1 electrolytes are evidenced in Figure 3. Figure 4a presents changes in the ionic conductivity as a function of reciprocal temperature for $\text{P(EO)}_{10}\text{LiI}$ solid electrolytes with various content of calixarene. At temperatures below $30\text{ }^{\circ}\text{C}$, conductivities obtained for electrolytes with $x = 0.05, 0.10$, and 0.20 are higher than for the pristine $\text{P(EO)}_{10}\text{LiI}$

(37) Fuoss, R. M.; Accascina, F. *Electrolytic Conductance*; Interscience: New York, 1959.

(38) Huang, W.; Frech, R.; Wheeler, A. J. *Phys. Chem. B* **1994**, *98*, 100.

(39) Cruickshank, J.; Hubbard, H. V.; Boden, St. A.; Ward, I. M. *Polymer* **1995**, *36*, 3779.

(40) Zalewska, A.; Stygar, J.; Ciszewska, E.; Wiktorko, M.; Wieczorek, W. *J. Phys. Chem. B* **2001**, *105*, 5847.

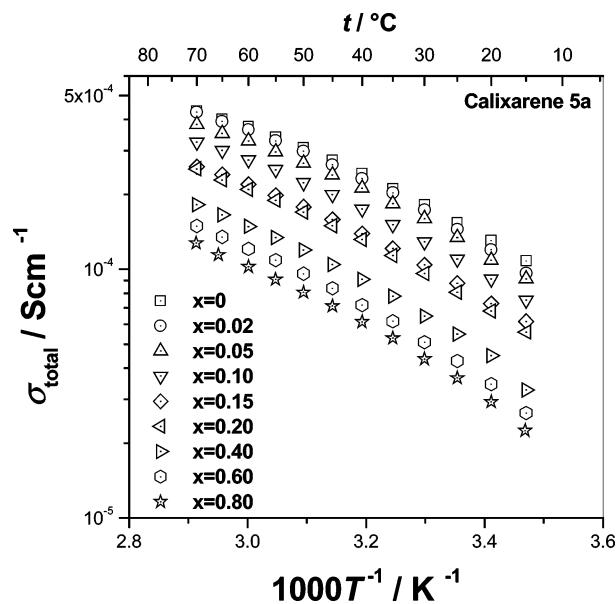


Figure 2. Temperature dependence of conductivity for the P(EO)DME₁₀₀-(LiI)₁(calixarene)_x electrolyte.

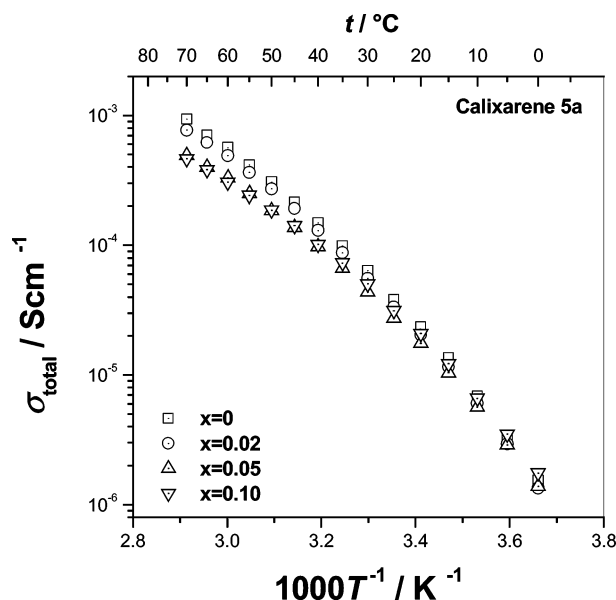


Figure 3. Temperature dependence of conductivity for the P(EO)DME₁₀-(LiI)₁(calixarene)_x electrolyte.

electrolytes. At temperatures above the melting point of the crystalline phase, conductivity of the P(EO)₁₀LiI electrolyte is the highest. On each curve, one may distinguish two intervals, in which the dependence of conductivity on temperature can be fitted with the Arrhenius type equation

$$\sigma = \sigma_0 \exp\left(-\frac{E_a}{k_B T}\right) \quad (2)$$

where E_a is an activation energy for effective ionic conduction in electrolyte, σ_0 is the pre-exponential factor including information about concentration of mobile ions and the entropy of ionic migration, and k_B denotes Boltzmann's constant. The point of inflection on each curve corresponds approximately to the melting temperature of the eutectic or crystalline P(EO) phase. The temperature dependencies of ionic conductivity have been fitted separately using eq 2 for

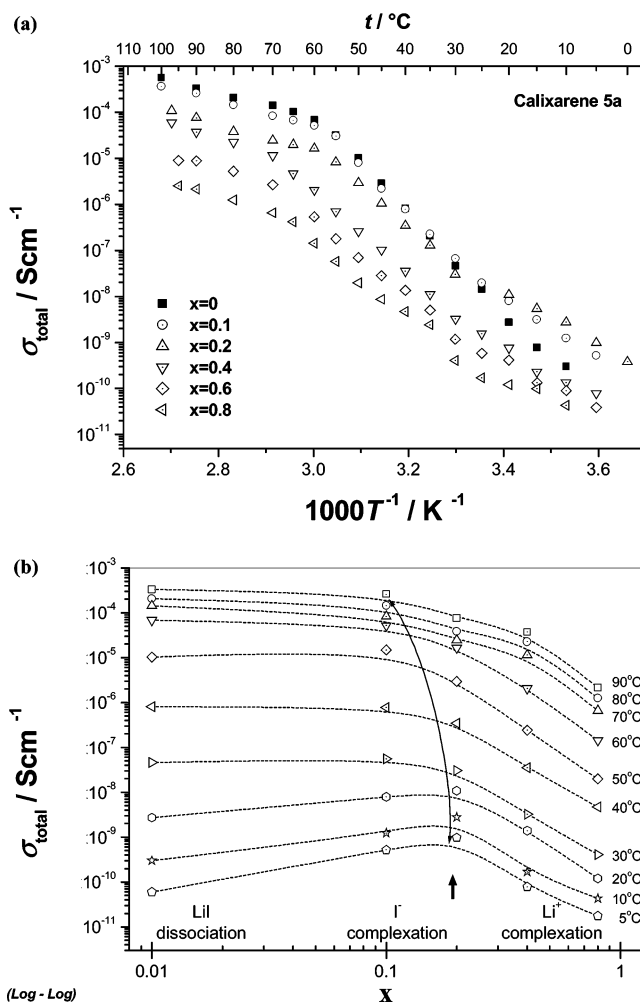


Figure 4. (a) Temperature dependence of conductivity for the P(EO)₁₀-(LiI)₁(calixarene)_x solid electrolyte and (b) conductivity isotherms in the log-log representation. Particular ranges are hypothetically associated to calixarene induced salt dissociation, anionic and also cationic complexation.

the two intervals mentioned above. The values of activation energy calculated according to this procedure are included in Table 1. Generally, the activation energy at the lower regime is higher than at temperatures above the melting point. The addition of calixarene significantly lowers the activation energy at the low-temperature region, whereas above the melting point of the crystalline phase, the activation energy for P(EO)₁₀LiI electrolyte is ca. 0.1 eV lower than that of electrolytes with calixarene additives.

By assumption that the activation energy consists of both the ion creation and migration terms,⁴¹ and taking into consideration that above the melting point the migration is predominant,⁴² it can be concluded that the addition of calixarene results in a decrease of the activation energy for creation of charge carriers and an increase in the activation energy for ionic migration.

As evidenced from Figure 4b, in solid polymer electrolytes, at temperatures below 40 °C, the addition of calixarenes up to $x = 0.2$ results in an increase in the total conductivity, what is particularly advantageous for samples with high LiI content of O:Li ratio 10:1. That could be attributed to an

(41) Siekierski, M.; Wiczeorek, W. *Solid State Ionics* **1993**, 60, 67.

(42) Wiczeorek, W. *Solid State Ionics* **1992**, 53–56, 1064.

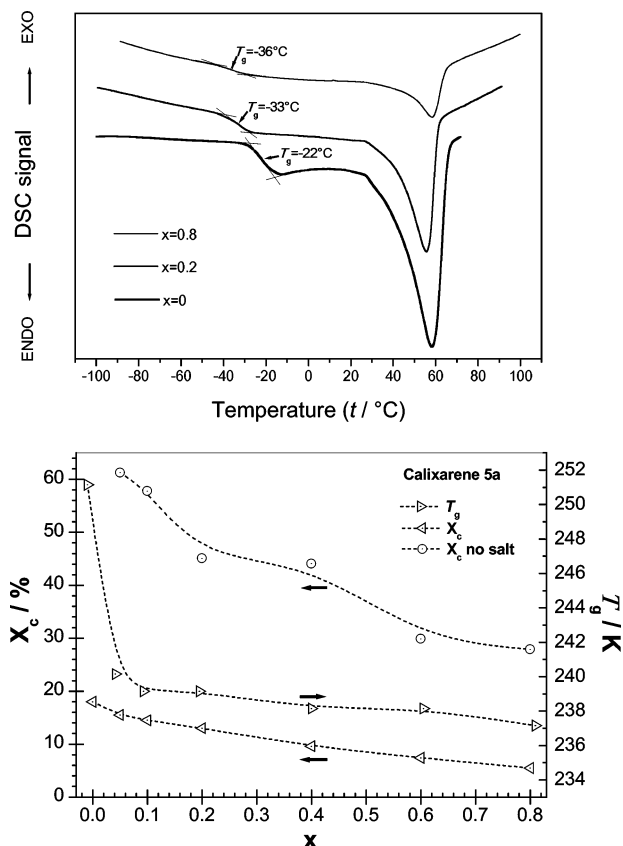


Figure 5. (a) Differential scanning calorimetry traces for the solid P(EO)₁₀-(LiI)₁(calixarene)_x system at various additive content ($x = 0$ and 0.2), heating from -100 to 100 °C at 20 °C/min. (b) The effect of calixarene content on T_g and X_c . Dashed lines are guiding eyes.

improvement in ionic dissociation related to the calixarene complexation. Above $x = 0.2$, conductivity generally decreases. At temperatures above 40 °C, the decrease in conductivity is observed in all the entire x range, which is due to a “removal” of mobile charge carriers (anions) from the well-dissolved salt by calixarene.

Table 2 shows the values of glass transition temperature T_g based on DSC experiments as a function of calixarene concentration for P(EO)DME electrolytes with O:Li ratio 100:1 and 10:1. For comparison, the T_g values obtained for P(EO)₁₀(LiI)₁(calixarene)_x solid electrolytes are also shown in Table 2. For the 100:1 electrolytes, T_g increases with the calixarene concentration. This is in contrast to 10:1 electrolytes (either of low or high molecular weight polyethers). Figure 5 shows the effect of calixarene content on the T_g values and degree of crystallinity (X_c) for P(EO) electrolytes. The X_c value is calculated from ratio of the latent melting heat (Q_m) for the polyether used to the latent melting heat found for the crystalline P(EO) phase

$$X_c = \frac{Q_m}{Q_{m\text{PEO}}} \quad (3)$$

where $Q_{m\text{PEO}} = 213.7$ J/g.^{43,44} As one may see, X_c decreases as the calixarene concentration increases. For comparison, DSC data for P(EO)–calixarene (no LiI) system are shown

in Table 3. In this case, opposite to X_c , T_g increases with calixarene content. The X_c calculated for doped and undoped systems is normalized in respect to pure P(EO). The apparently opposite trends in T_g dependence on calixarene content in the case of highly doped (Table 2) and undoped (Table 3) systems reflects interaction between calixarene and salt. This may also indicate on steric hindrance causing by calixarene, which leads to a lower degree of polymer crystallinity.

Table 4 contains FTIR data for P(EO)DME₁₀₀LiI and P(EO)DME₁₀LiI electrolytes modified with various amounts of calixarene. Two regions of the spectra, a response of the polymer matrix and the calixarene receptor, respectively, are analyzed. In the case of low calixarene content, in 100:1 electrolytes, the polyether C–O–C mode initially downshifts. The upshift is observed for the systems with higher salt concentration. Such a trend suggests weakening of the ion matrix and strengthening of the ion–ion interactions, what leads to a general decrease in the transient cross-link density. In the case of calixarene N–H stretching vibrations, changes are not pronounced for 100:1 electrolytes. There is more apparent upshift of both peaks maxima with an increase in calixarene content for 10:1 electrolytes. The mode splitting can also be observed (see Table 4). The difference in the hydrogen-bonded stretching frequencies of calixarene peaks is 31 (with 0.05) and 26 wavenumbers (with 0.1 calixarene content); it results from the difference between two urea hydrogens of different acidity determined by both calixarene substituents (*n*-butyl and phenyl).

The above trends confirm the ability to form strong hydrogen bonding to iodide anions by calixarene derivatives. FTIR data corresponds to DSC observations.

3.2. Lithium Ion Transference Number. Before measurement of the lithium transference number t_+ , stability of the electrolyte–electrode interface should be tested. For corresponding results related to systems described in this and our previous paper,⁴⁵ see Appendix 1. Our studies demonstrate that there are no changes in the interfacial resistance upon time and, therefore, justify the use of ac/dc technique for the evaluation of t_+ (see Table 5).

As can be seen for O:Li = 100:1 samples, t_+ remains almost unchanged regardless of calixarene **5a** addition, while for 20:1 samples, a considerable increase from 0.35 up to 0.59 in the case of electrolyte with calixarene concentration $x = 0.3$ is followed by a decrease down to again nearly 0.35 at $x = 1$. That would suggest a possibility to complex beside anions also cations by calixarene **5a**.

Further in Table 5, there are t_+ values presented for concentrated electrolytes (O:Li = 20:1 or 7:1) as a function of calixarene **5c** content and the type of anion used. The addition of calixarene **5c** (or **5b**) into the (PEO)₇LiI electrolyte results in the increase in t_+ even above 0.7 for $x = 0.3$ (it should be stressed that in this case we were unable to synthesize homogeneous electrolytes with calixarene-to-salt ratio higher than 0.3). For comparison, data obtained for (PEO)₂₀LiCF₃SO₃ electrolyte with and without calixarene

(43) Li, X.; Hsu, S. L. *J. Polym. Sci., Polym. Phys. Ed.* **1984**, 22, 1331.

(44) Przyłuski, J.; Wiczeorek, W. *J. Thermal Analysis* **1992**, 38, 2229.

(45) Blażejczyk, A.; Wiczeorek, W.; Kovarsky, R.; Golodnitsky, D.; Peled, E.; Scanlon, L. G.; Appetecchi, G. B. and Scrosati, B. *J. Electrochem Soc.* **2004**, 151 (10), A1762.

additive are also shown in order to point up both a possibility to complex various anions by the same receptor and the significant increase in t_+ up to 0.9 following addition of calixarene **5c** agent.

In the case of electrolytes with I^- anions, the effect of salt content and temperature on t_+ may also be derived from the data. Commonly, the higher the salt concentration (in respect to matrix), the higher the t_+ value. That is apparent reflecting the complexation phenomenon dependence on ion-ion and ion-matrix interactions, which compete with anion binding by receptors. It can be noticed that in general t_+ value decreases with an increase in temperature. For the electrolytes including calixarene **5c** with the additive to salt molar ratio 1:1 at 50 °C, the highest Li^+ transference number equal to unity is achieved.

4. Discussion

We have studied receptor systems based on *p-tert*-butyl-calix[4]arene embedded with various neutral urea moieties (compounds **5a–c**), which are capable of sensing and coordinating halogen anions, as discovered by Reinhoudt's (**5a**)³⁰ and our groups (**5b,c**).⁴⁵ Their complexing performance has been investigated in the lithium salt polyether based electrolyte environment. Since neither chloride nor bromide salts can be dissolved in polyether, the whole data set acquired concern mostly the iodide anion electrolytes.

The consideration on the potential usage of the calixarene additive in lithium polyether electrolyte cells led us to the following preclusions. First, in such supramolecules immersed in the electrolyte environment, strong hydrogen anion-receptor bonds (competitive to anion-solvent, anion-cation, and other interactions) can be easily formed. Second, the receptors meet the requirement of low protonic acidity,⁴⁶ which (if too high) could contribute to passivation of the lithium electrode. Adding calixarene may then simultaneously both effectively "purify" the electrolyte from associated and mobile anions, what also restricts passive layer forming in polarized cell, and (by this) help suppress the progressive growth of the SEI layer. The relatively stable SEI and the double-layer absence should make Li^+ charge electrode-electrolyte transfer "easier", which also confirms a relative increase in the transference number $t_+ \approx t_{Li+}$. The above expectation has been confirmed in the low-frequency impedance and long time current experiments performed in the symmetrical Li/solid-electrolyte//Li cells (see Appendix 1 for interpretation details).

The effectiveness of anion-receptor complexing in the electrolytes under study we derived experimentally both from the t_+ measurement results and FTIR signals. As shown in Figure 1, the addition of calixarene (at O:Li constant) resulted in a general decrease of the total ionic conductivity. In the view of DSC data (Table 2), such a trend can be also attributed to anion complexing phenomenon rather than, e.g., to a decrease of fluidity or increase in electrolyte viscosity, which indeed falls down when augmenting calixarene content (regardless of its macromolecular nanoscale dimensions).

On the basis of the experimental results, the following ionic transport mechanism in polyether electrolyte modified with calixarene additives could be deduced. The calixarene interacts preferably with iodide anions rather than lithium cations, what apparently has a positive effect on the cationic to anionic conductivity constituents' ratio. In the case of lowest LiI salt concentrations, intramolecular cross-links coordinating cation to polyether oxygens dominate. That is associated with trapping of mobile cations inside the potential wells, so their transport is relatively poor. In these electrolytes, any addition of calixarene has an insignificant effect on the cation transport number (see t_+ for 100:1 in Table 5); on the other hand, the drop in conductivity is remarkable (compare Figures 1 and 2). This behavior may be explained through the fact that complexing anions by calixarene additives directly leads to a remarkable increase in cation-matrix interactions. Evidently, most of the anions are "swallowed" and probably well screened by urea moieties in calixarene receptors, thus, the "shielding salt environment" does no longer exist from the (exposed to PEO oxygen traps) cations' point of view. That must lead to a significant drop in cationic mobility. Additionally, the presence of a bulky supramolecular additive acts as a steric hindrance for segmental motions of polyether chains, what may also impede both the cationic and anionic (if still present) transport. The evidence for that is the increase in the T_g values and hindering the material crystallinity in this set of polymer electrolytes (see Tables 2 and 3 and Figure 5).

The above analysis strongly suggests consideration of the future using somewhat less complex anion-binding receptors of more open conformation (such as calixpyrrole⁵⁴ or, even much simpler, directly grafted to polymer chains²⁷ or "small but heavy"), so beside immobilization of anions (together with receptors), cations could still interact with their counterparts (cation-anion ionic bonds would not be then disrupted).

In the case of highest LiI salt concentration, intermolecular cross-links via positively charged triplets linking the polyether chains dominate. Moreover, addition of calixarene

(46) Bordwell, E.; Algrim, D. J.; Harrelson, J. A. *J. Am. Chem. Soc.* **1988**, *110*, 5903.

(47) (a) Garbarczyk, J. E.; Wasiucionek, M.; Machowski, P.; Jakubowski, W. *Solid State Ionics* **1999**, *119*, 9. (b) Machowski, P.; Garbarczyk, J. E.; Wasiucionek, M. *Solid State Ionics* **2003**, *157*, 281.
(48) Vines, J.; Böhrer, V. *Calixarenes, a Versatile Class of Macrocyclic Compounds*; Kluwer Academic Press: Dordrecht, 1991; Vol. 3.
(49) Gutsche, C. D.; Bauer, L. J. *J. Am. Chem. Soc.* **1985**, *107*, 6052.
(50) (a) van Loon, J. D.; Verboom, W.; Reinhoudt, D. N. *Org. Prep. Proc. Int.* **1992**, *24*, 437. (b) van Dienst, E.; Bakkeer, W. I.; Engbersen, J. F. J.; Verboom, W.; Reinhoudt, D. N. *Pure Appl. Chem.* **1993**, *65*, 387.
(51) (a) Gutsche, C. D.; See, K. A. *J. Org. Chem.* **1992**, *57*, 4527. (b) van Loon, J. D.; Janssen, R. G.; Verboom, W.; Reinhoudt, D. N. *Tetrahedron Lett.* **1992**, *33*, 5125. (c) Murakami, H.; Shinkai, S. *J. Chem. Soc., Chem. Commun.* **1993**, 1533.
(52) (a) Shinkai, S.; Fujimoto, K.; Otsuka, T.; Herman, H. L. *J. Org. Chem.* **1992**, *57*, 1516. (b) Arnaud-Neu, F.; Barrett, G.; Harris, S. J.; Owens, M.; McKervey, M. A.; Schwing-Weill, M. J.; Schwinte, P. *Inorg. Chem.* **1993**, *32*, 2644.
(53) (a) Beer, P. D.; Dickson, C. A. P.; Fletcher, N.; Goulden, A. J.; Grieve, A.; Hodacova, J.; Wear, T. *J. Chem. Soc., Chem. Commun.* **1993**, 828. (b) Morzherin, Y.; Rudkevich, D. M.; Verboom, W.; Reinhoudt, D. N. *J. Org. Chem.* **1993**, *58*, 7602. (c) Beer, P. D.; Chen, Z.; Goulden, A. J.; Stokes, S. E.; Wear, T. *J. Chem. Soc., Chem. Commun.* **1993**, 1834.
(54) (a) Turner, B.; Shterenberg, A.; Kapon, M.; Suwiska, K.; Eichen, Y. *Chem. Commun.* **2001**, 13. (b) Gale, P. A.; Sessler, J. L.; Kral, V. and Lynch, V. *J. Am. Chem. Soc.* **1996**, *118*, 5140.

results in breaking of the triplet links by taking out the iodide anion. That in turn frees some mobile cations and also decreases the T_g values of the electrolyte. Both effects result in the conductivity and cation transference number enhancement (see Figures 3 and 4 and Table 5). The results do not depend on the molecular weight of the polyether used. The above assumptions were confirmed by studies on Li^+ conduction which revealed an increase in lithium transference number in the case of $\text{O}:\text{Li} = 20:1$ electrolytes containing $x = 0.3$ of calixarene **5a**. Interestingly, for higher calixarene concentrations, lithium transference number decreases. Likewise, it might be connected to the possible cation complexation either by polyether chains or calixarene oxygen centra.

One of the major goals of this study was to analyze the effect of various functional groups in urea calix[4]arene (**5a–c**) on complexation of anions used in electrolytes, toward chemical “programming” of requested transport properties. In the ideal chemically “programmable” case of receptor microstructure, the hydrogen bond donating site should be compatible with anion in terms of its geometry and charge distribution. The results discussed herein indicate that, to achieve selective anion binding, correct positioning of the hydrogen bond donating sites is crucial and is possible via application of appropriate substituents. By assumption that anion complexation occurs in the cage placed between active urea protons, the application of electron-donating bulky *tert*-butyl groups might result in some enlargement of the molecular cage of the receptor, which could improve its complexation ability toward anions. On the other hand, an increase in protonic acidity should also enlarge the complexation constant. Therefore, the use of electron-accepting functional groups such as *p*-nitrophenyl could be expected to cause better complexation of anions. And indeed, the stronger electron-withdrawing nature of the *p*-nitrophenyl compared to phenyl substituent made chemical shift of urea hydrogens in the presence of the anion-free solution more downfield (see ^1H NMR data). Moreover, in the polyether electrolyte environment, the receptor **5c** provides perfect anion binding. This effect is clearly expressed in terms of data shown in Table 5, where t_+ tends to unity in the final case of $(\text{PEO})_{20}\text{LiI}$ –calixarene **5c** electrolyte.

To our knowledge, this is the first time the lithium transference number t_+ is found equal to unity as obtained for high molecular weight solid polyether electrolyte.

Concluding, similarly, e.g., to the case of other mixed electron–ionic conductors,⁴⁷ fine-tuning chemical composition and particularly microstructure of supramolecular additives, makes feasible modifying polymer electrolyte properties in terms of ionic transport from almost anionic through mixed (of equal contributions of anions and cations to conductivity) up to purely cationic (of transference number equal 1) within the same polymer system. The result constitutes a “significant advance” that could be of a broader interest to material scientists.

5. Summary

New supramolecular compounds calix[4]arene R-urea derivatives ($\text{R} = \text{phenyl}, t\text{-butyl}, p\text{-nitrophenyl}$) have been

designed, synthesized, and used as neutral anion-binding receptors in polyether electrolytes.

It has been established that most properties of the system studied do not depend on molecular weight of the polymer matrix used but are rather sensitive to microstructure and concentration of the additive.

On the basis mainly of ac impedance, dc current, FTIR, and DSC analysis, we have concluded some details concerning ionic transport in lithium cell. Changes in the electrolyte conductivity and t_+ were associated to complexation of anions by calixarene receptors, causing considerable modification of the transport mechanism from almost anionic through mixed (equal contributions of anions and cations to conductivity) to purely cationic (transference number equal 1). Also, the addition of the supramolecular compounds has been found to suppress growth of secondary passive layers. Their nature has been discussed (see Appendix 1) in terms of impurities and salt precipitation.

Acknowledgment. This work was partially supported by U.S. Air Force Research Office (under the 500/N/1020/0902 research contract). Research contained in this paper was performed in partial fulfillment of the Ph.D. and M.Sc. requirements in Solid State Technology Division, Faculty of Chemistry at Warsaw University of Technology. One of the authors, A.B., would like to thank Dr. P. Machowski for helpful discussion on transference number measurements as also students from Warsaw University of Technology for their help in due course of organic synthesis.

Appendix 1

Why Calixarene Derivatives as Additives for Polymer Electrolyte?

Generally, synthetic anion receptors reveal relatively modest selectivity. Should one design “intelligent” anion receptors of higher selectivity and anion affinity, one may need to develop a specific strategy to position various anion binding sites on a molecular platform. Such a platform must exhibit some special characteristics, i.e., to have a certain degree of preorganization and allow functionalization in a simple way. The family of calix[4]arenes satisfied these conditions. Calixarenes provide a unique platform for the supramolecular chemist to build on.⁴⁸ The interest in calixarenes has grown rapidly because of numerous derivatives that can be created via relatively simple synthesis and because of their appealing three-dimensional symmetry. Of particular interest are derivatives of the tetramer, which in their cone conformation⁴⁹ are characterized by (i) the hydrophobic cavity, located between the aromatic rings of the *p*-substituted phenolic units (known to interact with neutral species) or (ii) the hydrophilic cavity, resulting from introduction of the functionalized phenolic OH groups (lower rim) or from selective functionalization⁴⁹ at the para positions of phenol rings (upper rim). Since their semirigid 3D structure allows binding sites to be matched with size and shape of the target, the cavities are able to recognize some neutral molecules,⁵¹ cations,⁵² or anions⁵³ selectively. The upper and lower rims are easily modifiable with a large variety of functional groups. That allows for building a wide

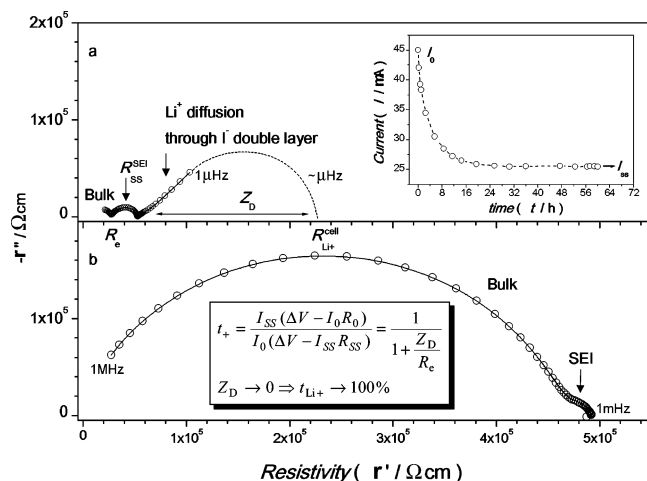


Figure 6. Impedance response and dc current measurement of the symmetrical Li/PE/Li cell at 55 °C: (a) in the case of P(EO)₂₀LiI electrolyte, (b) in the case of P(EO)₂₀(LiI)₁(calixarene 5c)₁ modified electrolyte. Dashed lines are guides for the eye. The lowest frequency response, of the shape corresponding (via Fourier transformation) to the long-time dc measurement (see inset), has been extrapolated to illustrate the diffusive process of Li⁺ charge transfer through the “double layer” formed by a linear gradient of I⁻ anion concentration. Note, beside the increase in electrolyte resistivity, that the apparent Warburg response and the expected “semicircle” diameter Z_D tends to zero at calixarene content $x = 1$. The Z_D magnitude has been estimated regarding reasonable for polymer electrolytes assumption for t_+ as not lower than 0.1. The second inset refers to the Li⁺ transference number determination (see section 2.3.3).

range of structures either for binding or to enhance receptor solubility, both being of great importance for membrane ionic transport, beside other applications. On the other hand, it makes feasible developing basic models to elucidate further the fundamental aspects of anion coordination chemistry.

Particularly, in every synthesized calix[4]arene R-urea derivative under study, the urea hydrogen atoms could be designed to form an open arrangement of four dipoles (placing the maximum of positive potential in the center of cavity) which might help to set up (stronger than Coulombic) hydrogen bonding with anions. In our case, we could observe complexing anions of extremely different geometries by the same receptor (see results for 5c in Table 5). Despite small differences in effectiveness of complexation due to the geometry mismatch, we may then consider the phenomenon of anionic complexation by calixarene receptors as depending mostly on their ability to create hydrogen bonds with anions, and thus, we may concern the anionic site as “universal” in the certain range. Unlike other receptors, such as, e.g., calix[6]pyrrole,⁵⁴ the calixarene “anion-binding site” (see Scheme 1) prefers hosting one I⁻ anion per site, which leads to stoichiometry of binding to be 1:1 when forming complexes within polymer electrolytes.³⁰ The latter calixarene feature enables estimating changes of mobile charge carriers’ fraction due to complexing anions in the mixed ionic polymer conductor. Yet, one has to take into account that ability to bind an anion might compete with effective polarizability of a solvent in electrolyte.^{30,54}

By consideration of the above-mentioned advantages, these receptors could be applied as supramolecular additives into a polyether electrolyte in order to make cationic transport dominate over anionic. Moreover, the approach was supported by the fact that anion-binding urea hydrogens do not reveal high acidity, which otherwise in the case of potential

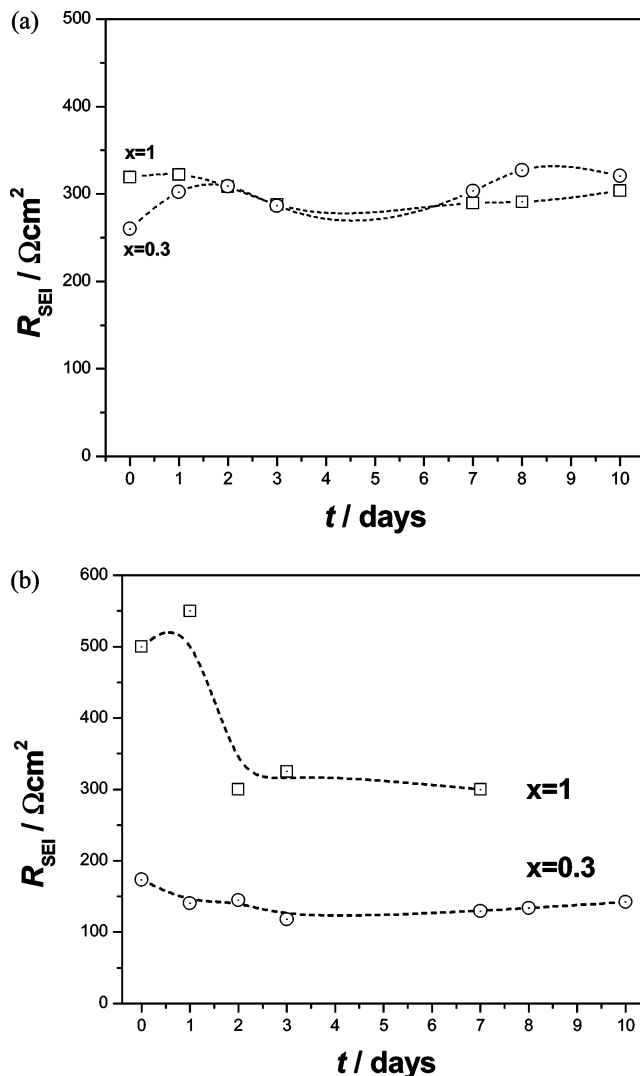


Figure 7. Time evolution of the SEI passivating resistance R_{SEI} at 50 °C in the Li/(P(EO)₂₀:(LiI)₁:(calixarene)_{*x*})/Li cell for (a) calixarene 5a and (b) 5c at $x = 0.3$ and 1.

application could affect the lithium battery anode. Regarding progressive degradation of the electrode–electrolyte interface, we will now discuss the question how does it benefit from the use of anion-binding calixarene receptor as additive to the lithium cell?

Interfacial Stability. The stability of the so-called solid electrolyte interface (SEI), which is supposed to include a (so far not precisely defined) layer between lithium electrode and the polymer electrolyte, has been measured by means of IS in the symmetric cell (Figure 6). Figure 7 presents typical time dependence of the SEI resistance taken from the impedance spectra on the example of electrolytes containing (in respect to LiI) $x = 0.3$ and $x = 1$ for calixarenes 5a (Figure 7a) and 5c (Figure 7b).

As can be deduced, the initial SEI layer might originate and is progressively formed from both chemical impurities (either dispersed in electrolyte or stored on surfaces) and, more likely, salt precipitation from the electrolyte to the internal electrode surface. Its passivating Li⁺ transfer resistance apparently depends on the type and concentration of calixarene derivative. This resistance ($\sim 10^2$ Ω) is usually observed to be a little higher than that of the pristine

(PEO)₂₀LiI electrolyte. On the other hand, the secondary interfacial resistance R_{SEI} was found to be stable for long time periods up to 250 h at 50 °C, independently on the composition. Although, more precise cyclic voltammetry (CV) measurements on shorter time periods would be required to confirm the detected effect of stabilization, we may already conclude that usually observed progressive growth of the passive layer can be definitely suppressed by using the calixarene-based electrolyte membranes. The observed effect can be understood in terms of the complexing phenomenon, by which immobilized anions are restricted from the formation of interfacial double layer on polarization of the cell (compare Warburg impedances⁵⁶ and Z_D ⁵⁷ in parts a and b of Figure 6), which we believe mainly accelerates growth of the secondary SEI layer through subsequent salt precipitation on the lithium electrode surface. In this context, observed stabilization of the interface, as well as apparent disappearance of the double layer polarization, would be the strong evidence for iodide anion–calixarene receptor complexing in the polyether environment.

Appendix 2

The data (¹H NMR, ¹³C NMR, IR, MS, Anal. Calcd, mp) obtained in this study are presented as follows.

1. ¹H NMR (CDCl₃, 500 MHz, ppm) δ : 1.21 (s, 36H, (CH₃)₃), 3.49 (d, J = 13.5, 4H, Ar–CH₂–Ar, eq), 4.26 (d, J = 13.4H, Ar–CH₂–Ar, ax), 7.05 (s, 8H, ArH), 10.34 (s, 4H, OH).

IR (neat, cm^{−1}): ν_{OH} 3139, ν_{C-OH} 1201. Mp (°C): 333–335 in this case for the complex with toluene. Anal. Calcd for C₄₄H₅₆O₄ (648.91): C, 81.44; H, 8.70. Found: C, 81.57; H, 8.77.

2. ¹H NMR (CDCl₃, 400 MHz, ppm) δ : 1.02 (s, 18H, (CH₃)₃), 1.27 (t, J = 7.6, 6H, CH₃), 1.28 (s, 18H, (CH₃)₃), 1.99–2.09 (m, 4H, CH₂), 3.31 (d, J = 13.2, 4H, Ar–CH₂–Ar, eq), 3.95 (t, J = 6.4, 4H, OCH₂), 4.33 (d, J = 12.8, 4H, Ar–CH₂–Ar, ax), 6.86 (s, 4H, ArH), 7.04 (s, 4H, ArH), 7.88 (s, 2H, OH).

¹³C NMR (CDCl₃, 400 MHz, ppm) δ : 10.85 (CH₃), 23.43 (CH₂CH₃), 31.07, 31.69 (C(CH₃)₃), 31.85 (Ar–CH₂–Ar), 33.78, 33.96 (C(CH₃)₃), 78.06 (OCH₂), 125.04, 125.46 (3°Ar–H), 127.74, 132.87 (4°Ar–CH₂), 141.65, 146.65 (4°Ar–(CH₃)₃), 149.95 (4°Ar–OCH₂), 150.82 (4°Ar–OH). IR (neat, cm^{−1}): ν_{OH} 3394, ν_{C-OH} 1210, $\nu_{C-O-C_{asym}}$ 1196, $\nu_{C-O-C_{sym}}$ 1062. Mp (°C): 238–240. MALDI-TOF: m/z 734.8 [M + H]⁺ (733.07 calcd), m/z 757.1 [M + Na + H]⁺ (757.07 calcd). Anal. Calcd for C₅₀H₆₈O₄ (733.07): C, 81.92; H, 9.35. Found: C, 81.81; H, 9.49.

3. ¹H NMR (CDCl₃, 400 MHz, ppm) δ : 0.94 (t, J = 7.6, 6H, CH₃), 1.03 (s, 18H, (CH₃)₃), 1.11 (s, 18H, (CH₃)₃), 1.77–1.84 (m, 4H, CH₂), 1.95–2.10 (m, 8H, CH₂), 3.10 (d, J = 12.8, 4H, Ar–CH₂–Ar, eq), 3.77 (t, J = 7.6, 4H, NCH₂), 3.81 (t, J = 7.6, 4H, OCH₂), 3.86 (t, J = 7.6, 4H, OCH₂),

4.37 (d, J = 12.4, 4H, Ar–CH₂–Ar, ax), 6.71 (s, 4H, ArH), 6.81 (s, 4H, ArH), 7.69–7.71 (m, 4H, ArH), 7.80–7.83 (m, 4H, ArH).

¹³C NMR (CDCl₃, 400 MHz, ppm) δ : 10.23 (CH₃), 23.43 (CH₂CH₃), 25.35, 27.55 (CH₂CH₂), 31.05 (Ar–CH₂–Ar), 31.39, 31.48 (C(CH₃)₃), 33.75, 33.82 (C(CH₃)₃), 37.98 (NCH₂), 74.51, 76.89 (OCH₂), 123.14, 133.78 (3°ArH–substit), 124.82, 124.95 (3°ArH–calix), 132.21 (4°ArH–substit), 133.47, 134.02 (4°ArH–CH₂), 144.20, 144.28 (4°Ar–(CH₃)₃), 153.23, 153.76 (4°Ar–O), 168.30 (C=O).

IR (neat, cm^{−1}): $\nu_{C=O}$ 1773, 1717, ν_{C-N} 1242, $\nu_{C-O-C_{asym}}$ 1202, $\nu_{C-O-C_{sym}}$ 1045. Mp (°C): 175–178. ESI: m/z 1158.4 [M + Na]⁺ (1158.51 calcd). Anal. Calcd for C₇₄H₉₀N₂O₈ (1135.52): C, 78.27; H, 7.99; N, 2.47. Found: C, 77.96; H, 8.10; N, 2.47.

4. ¹H NMR (CDCl₃, 400 MHz, ppm) δ : 1.01 (t, J = 7.6, 6H, CH₃), 1.04 (s, 18H, (CH₃)₃), 1.11 (s, 18H, (CH₃)₃), 1.51–1.60 (m, 4H, CH₂), 1.80 (br. s, 4H, NH₂), 1.94–2.10 (m, 8H, CH₂), 2.79 (t, J = 7.2, 4H, NCH₂), 3.11 (d, J = 12.4, 4H, Ar–CH₂–Ar, eq), 3.78 (t, J = 7.6, 4H, OCH₂), 3.90 (t, J = 7.6, 4H, OCH₂), 4.39 (d, J = 12.4, 4H, Ar–CH₂–Ar, ax), 6.72 (s, 4H, ArH), 6.82 (s, 4H, ArH).

¹³C NMR (CDCl₃, 400 MHz, ppm) δ : 10.46 (CH₃), 23.42 (CH₂CH₃), 27.57, 30.44 (CH₂CH₂), 31.07 (Ar–CH₂–Ar), 31.39, 31.48 (C(CH₃)₃), 33.75, 33.83 (C(CH₃)₃), 42.39 (NCH₂), 74.86, 77.20 (OCH₂), 124.81, 124.97 (3°ArH–calix), 133.44, 134.04 (4°ArH–CH₂), 144.17, 144.35 (4°Ar–(CH₃)₃), 153.45, 153.65 (4°Ar–O). Mp (°C): uncorrected. MALDI-TOF: m/z 875.3 [M]⁺ (875.32 calcd), m/z 897.9 [M + Na]⁺ (898.30 calcd). Anal. Calcd for C₅₈H₈₆N₂O₄ (875.32): C, 79.59; H, 9.90; N, 3.20. Found: C, 77.13; H, 9.75; N, 3.21.

5a. ¹H NMR (CDCl₃, 400 MHz, ppm) δ : 0.82 (s, 18H, (CH₃)₃), 0.98 (t, J = 7.2, 6H, CH₃), 1.33 (s, 18H, (CH₃)₃), 1.47–1.58 (m, 4H, CH₂), 1.79–1.90 (m, 4H, CH₂), 2.15–2.26 (m, 4H, CH₂), 3.11 (d, J = 12.4, 4H, Ar–CH₂–Ar, eq), 3.34–3.39 (m, 4H, NCH₂), 3.62 (t, J = 7.2, 4H, OCH₂), 3.98 (t, J = 8.0, 4H, OCH₂), 4.36 (d, J = 12.4, 4H, Ar–CH₂–Ar, ax), 5.91 (br. t, 2H, CH₂NH), 6.45 (s, 4H, ArH), 6.96 (t, J = 7.2, 2H, ArH), 7.10 (s, 4H, ArH), 7.19 (t, J = 8.0, 4H, ArH), 7.26 (d, J = 7.6, 4H, ArH), 7.48 (br. s, 2H, C₆H₅NH).

¹³C NMR (CDCl₃, 400 MHz, ppm) δ : 10.82 (CH₃), 23.56 (CH₂CH₃), 26.79, 27.66 (CH₂CH₂), 31.02 (Ar–CH₂–Ar), 31.14, 31.72 (C(CH₃)₃), 33.54, 34.04 (C(CH₃)₃), 40.68 (NCH₂), 74.63, 77.50 (OCH₂), 120.18, 123.00, 129.01 (3°ArH–substit), 124.37, 125.43 (3°ArH–calix), 131.87, 135.55 (4°ArH–CH₂), 138.99 (4°ArNH), 143.88, 144.79 (4°Ar–(CH₃)₃), 152.49, 154.64 (4°Ar–O), 156.65 (C=O). Mp (°C): 239–242. MALDI-TOF: m/z 1113.80 [M]⁺ (1113.56 calcd), m/z 1136.98 [M + Na]⁺ (1136.55 calcd). Anal. Calcd for C₇₂H₉₆N₄O₆ (1113.56): C, 77.66; H, 8.69; N, 5.03. Found: C, 75.25; H, 8.72; N, 4.76.

5b. ¹H NMR (CDCl₃, 400 MHz, ppm) δ : 0.85 (s, 18H, (CH₃)₃), 1.04 (t, J = 7.2, 6H, CH₃), 1.29 (s, 18H, (CH₃)₃), 1.35 (s, 18H, (CH₃)₃), 1.44–1.54 (m, 4H, CH₂), 1.82–1.94 (m, 4H, CH₂), 2.11–2.23 (m, 4H, CH₂), 3.11 (d, J = 12.4, 4H, Ar–CH₂–Ar, eq), 3.25 (t, J = 8.0, 4H, NCH₂), 3.66 (t, J = 7.6, 4H, OCH₂), 3.96 (t, J = 8.4, 4H, OCH₂), 4.36 (d,

(55) McDonald, N. A.; Duffy, E. M.; Jorgensen, W. L. *J. Am. Chem. Soc.* **1988**, *110*, 5104.

(56) Thomas, M. G. S. R.; Bruce, P. G.; Goodenough, J. B. *Solid State Ionics* **1985**, *17*, 13.

(57) Macdonald, J. R. *J. Chem. Phys.* **1973**, *58*, 4982.

$J = 12.4$, 4H, Ar-CH₂-Ar, ax), 4.80 (br. s, 2H, C(CH₃)₃NH), 5.07 (br. s, 2H, CH₂NH), 6.48 (s, 4H, ArH), 7.05 (s, 4H, ArH).

¹³C NMR (CDCl₃, 400 MHz, ppm) δ : 10.87 (CH₃), 23.54 (CH₂CH₃), 26.92, 27.69 (CH₂CH₂), 29.68 (C(CH₃)₃), 30.99 (Ar-CH₂-Ar), 31.16, 31.68 (C(CH₃)₃), 33.54, 34.04 (C(CH₃)₃), 40.68 (NCH₂), 74.78, 77.41 (OCH₂), 124.41, 125.34 (3°ArH-calix), 132.09, 135.32 (4°ArH-CH₂), 143.88, 144.66 (4°Ar-(CH₃)₃), 152.60, 154.54 (4°Ar-O), 158.08 (C=O). Mp (°C): 222–224. ESI: m/z 1073.8 [M + H]⁺ (1073.58 calcd), m/z 1095.8 [M + Na]⁺ (1096.57 calcd), m/z 1111.8 [M + K]⁺ (1112.67 calcd). Anal. Calcd for C₆₈H₁₀₄N₄O₆ (1073.58): C, 76.08; H, 9.76; N, 5.22. Found: C, 76.00; H, 9.73; N, 5.29.

5c. ¹H NMR (CDCl₃, 400 MHz, ppm) δ : 0.82 (s, 18H, (CH₃)₃), 0.95 (t, $J = 7.6$, 6H, CH₃), 1.32 (s, 18H, (CH₃)₃), 1.58–1.67 (m, 4H, CH₂), 1.77–1.89 (m, 4H, CH₂), 2.22–3.00 (m, 4H, CH₂), 3.12 (d, $J = 12.8$, 4H, Ar-CH₂-Ar, eq),

3.44–3.49 (m, 4H, NCH₂), 3.62 (t, $J = 7.2$, 4H, OCH₂), 4.01 (t, $J = 8.4$, 4H, OCH₂), 4.35 (d, $J = 12.4$, 4H, Ar-CH₂-Ar, ax), 6.07 (br. s, 2H, CH₂NH), 6.44 (s, 4H, ArH), 7.10 (s, 4H, ArH), 7.47 (d, $J = 9.2$, 4H, ArH), 8.07 (d, $J = 9.2$, 4H, ArH), 8.14 (br. s, 2H, C₆H₄NH).

¹³C NMR (CDCl₃, 400 MHz, ppm) δ : 10.82 (CH₃), 23.57 (CH₂CH₃), 26.66, 27.52 (CH₂CH₂), 30.97 (Ar-CH₂-Ar), 31.12, 31.70 (C(CH₃)₃), 33.55, 34.06 (C(CH₃)₃), 40.73 (NCH₂), 74.49, 77.40 (OCH₂), 117.84, 125.33 (3°ArH-substit), 124.43, 125.49 (3°ArH-calix), 131.78, 135.48 (4°ArH-CH₂), 142.00 (4°ArNH), 144.03, 145.00 (4°Ar-(CH₃)₃), 152.33, 154.48 (4°Ar-O), 155.43 (C=O). Mp (°C): 234–236. ESI: m/z 1220.7 [M + H]⁺ (1203.55 calcd), m/z 1225.7 [M + Na]⁺ (1226.54 calcd), m/z 1241.6 [M + K]⁺ (1242.65 calcd). Anal. Calcd for C₇₂H₉₄N₆O₁₀ (1203.55): C, 71.85; H, 7.87; N, 6.98. Found: C, 71.74; H, 7.89; N, 6.95.

CM048679J